Prioritizing management options using a risk assessment for soil erosion based on GIS, remote sensing, and RUSLE. A case study of Midhagdu Watershed, Eastern Ethiopia.

Sultan Mohammed
Haramaya University
Gadisa Fayera Gemechu (gfeyewollega2016@gmail.com)
Salale University
Michael Aliyi
Yangzhou University
Tewekel Melese Gemechu
Ambo University

Research Article

Keywords: Soil erosion, Soil Loss Risk Factors, RUSLE, GIS, Remote Sensing, Midhagdu

Posted Date: July 21st, 2022

DOI: https://doi.org/10.21203/rs.3.rs-1877352/v1

Abstract

This study prioritises management options and assesses the risk of soil erosion in the Midhagdu Watershed in eastern Ethiopia. The themed map was developed using satellite data including SRTM-DEM, Landsat OLI, rainfall data, and soil data. The RUSLE model as well as GIS and remote sensing methods were used in the experiment. The experiments revealed that the factors that affect soil erosion risk such as rainfall erosivity (R), soil erodibility (K), slope length and steepness (LS), cover management (C), and anthropogenic soil erosion control practises factor values were distributed spatially and ranged in values from 41.365 to 43.793MJ mm ha-1yr-1, 0.26 to 0.31t ha-1MJ-1mm-1, 0 to 220.512, 0.21 to 0.87, and 0.11 to 1, respectively, and the most powerful factor that influences soil erosion risk was topography(LS) with a value of 0.885. The results of the grid cell-based RUSLE model showed that 52.24 percent of the Midhagdu watershed (28.37 km2 out of 54.3 km2) had low to moderate soil erosion levels and that 47.76 percent (25.94 km2 out of 54.3 km2) had high to extremely high soil erosion risk levels. By taking into account regions and priority classes based on soil erosion risk levels, the conclusions of this article suggest an early intervention to better plan soil erosion risk management.

1 Introduction

One of the biggest issues with land degradation around the world is soil erosion. Natural and controlled ecosystems are seriously endangered by soil erosion, which is frequently referred to as a geomorphological and land degradation process[1–3]. It is a natural process that changes according to both natural and man-made factors, leading to increased runoff from more impermeable subsoil, loss of nutrient-rich topsoil, decreased soil productivity, decreased biodiversity, and indirect environmental impact. While soil erosion is a common and long-lasting occurrence on Earth, it has gotten worse recently as a result of greater human involvement[4]. On the other hand, the reasons behind and consequences of soil erosion are intricate and multifaceted. Some of the main causes include population growth, bad governance, overuse of natural resources, and climate change[5–8]. The likelihood of food poverty rises as a result of soil erosion, which also reduces agricultural output globally and its long-term viability[9]. In order to assure adequate food supplies, many nations have turned to artificial fertilisers and pesticides. These factors affect the geochemical quality of the water, the biological and aquatic environments, and ground contamination[10]. The amount of vegetation available for food production around the world is reduced by about 10 million hectares per year due to soil erosion[11]. In Ethiopia's traditional farming communities, erosion is a common problem that has gotten worse recently as a result of increased human interaction[12, 13]. Cliffs, poor land use practises, violent storms, disrupting ground currents, floods, improper land management systems, and inadequate measures to prevent anthropogenic soil erosion in Ethiopia, which has significantly lower crop production in each region than global standards[14], are a few examples of anthropogenic and environmental activities that contribute to the erosion problem. To achieve food security, poverty reduction, and environmental sustainability, the Ethiopian government initiated a comprehensive land and water conservation (SWC) programme in the early 1970s[15, 16]. Land users' acceptance and persistence have been constrained for a variety of reasons despite major efforts to develop technology for soil and water conservation. Environmental studies for planning land use, land cover, and water management are increasingly using a geographic information system, remote sensing, and modelling tools[17].

Examples of parametric models for predicting soil erosion, assessing the extent of erosion, choosing the appropriate site and potential erosion risk, as well as prioritising identified soil erosion control alternatives, include the Revised USLE (RUSLE), Universal Soil Loss Equating (USLE), Modified USLE (MUSLE), GIS, and RS soil erosion risk assessment systems[9, 18]. Because it incorporates the influence of profile convexity (concavity) using segmentation of irregular slopes and an improved empirical equation for computing slope factor (LS)[19], the Revised Universal Soil Loss Equation (RUSLE) is one of the most well-liked contemporary models for estimating soil loss.

Due to deterioration of soil structures, chemistry, and biology, mostly as a result of rapid soil erosion and insufficient management strategies, the research site (Midhagdu watershed) is degraded and unproductive[20]. In order to effectively eliminate the risk of soil erosion and ensure sustainable environmental and socioeconomic development, it is crucial to provide strategies and access to contemporary geospatial data on the factors that contribute to soil erosion, erosion risk areas, erosion risk levels, and soil erosion prepared maps. In the Western Hararghe Highlands of Eastern Ethiopia, the Midhagdu Watershed is the focus of this study's investigation into soil erosion risk and the prioritisation of management options. The specific goals were to I identify the geographic distribution of soil erosion risk factors in the Midhagdu watershed, (ii) estimate the mean annual soil loss rate using the RUSLE watershed modelling software, and (iii) prioritise management options for soil conservation based on soil loss risk levels at micro watersheds within the Midhagdu watershed.

2 Materials And Methods

2.1 Details of the study area

Midhagdu watershed is part of the Fugug mountains of Western Hararge Chercher highlands, Ethiopia. Geographically, the watershed lies between 41^{0}5'0" E to 41^{0}7'30" longitude and 09^{0}10'0" N to 09^{0}15'0" N latitude, with a total area of 54.3km^2. The research region has an average elevation of 2130 metres above mean sea level and a range of elevations between 1760 and 2500 metres. characterised by bi-modal precipitation, with mean lowest temperatures of 12°C and maximum air temperatures of 26°C, and semiarid to subhumid agro-ecological zones (Tizita, 2016). 59 percent of the region is covered by leptosols, 26 percent by eutric cambisols, 8 percent by helpic zerosols, and 7 percent by eutric fluvisols, according to national digital soil data from 2014. Although there is irrigated agriculture in the watershed, it is predominately rain-fed agriculture, which is more unpredictable and short-lived and frequently experiences moisture stress. Land deterioration and soil erosion have a significant negative impact on agricultural production (CSA, 2007). To gather information from several sources and enhance the quality of the information during analysis and interpretation, a mixed research design or triangulation technique was adopted.

2.2 Sample data collection and analysis

Both primary and secondary data from various sources were used in the study. In order to collect both quantity and meaningful data, a variety of data gathering technologies were used to quantify and integrate triangular data sources. The primary secondary data sources used are the Ethiopian Ministries of Water, Irrigation, and Energy, as well as satellite images, soil data, rainfall data, and ground truth data (Table 1).

Table 1
Datasets used in the experiments

Datasets	Sources	Parameters
Landsat 8 OLI	https://glovis.usgs.gov	Land Use Land Cover (LULC), Normalized Difference Vegetation Index (NDVI)
Digital Elevation Model (30m X 30m)	Shuttle radar topographic mission (SRTM)	Slope
Climate data	Terraclimate	Rainfall
Soil data	MoWIE and FAO 1986	Soil texture

After pre-processing and image enhancement operations (density slicing, contrast correction, edge enhancement, and colour composite), satellite images like Landsat 8 OLI and SRTM-DEM were utilised to derive land use cover (LULC) data and Normalized Difference Vegetation Index (NDVI). A thorough field investigation was done to gather data on the main LULC types through direct and indirect field observation, GPS ground truth data collection, Google Earth image visualisation, and expert interpretation. To reduce salt-and-pepper effects, a 33 moving window majority filtering operation for neighbouring cells in classified LULC images was used. In ArcGIS 10.4, the watershed outflow point was used to automatically define the watershed boundary. Due to insufficient data, the Terraclimate universal free database supplied monthly rainfall calculated from long-term observations based on extrapolations of observed data indicative of 1988–2019 and retrievable [21]. The grid rainfall map included data on rainfall for each of the six stations—Chiro, Kuni, Shanan, Mullu, Afdem, and Deder—over the previous 31 years.

2.3 Soil erosion and soil erosion risk factors

The long-term average yearly rate of soil erosion was anticipated by the Revised Universal Soil Loss Equation (RUSLE) model. The most popular empirical model for determining soil loss per unit area is RUSLE [22]. As input factors, we employed slope length and steepness (LS), soil erodibility (K), rainfall erosivity (R), cover management (C), and support practise (P). The formula is typically written as follows (Renard et al. 1997):

$$A = R*K*LS*C*P (1)$$

Where: LS = the topographical factor (dimensionless), with the slope length factor (L) and the slope gradient (S) factor; P = the specific erosion control practises factor (dimensionless); and C = vegetation/land cover factor. Where: A = the average annual soil loss (in tonne $ha^{-1}yr^{-1}$); R = the rainfall and runoff erosivity (in $MJ.mm.ha^{-1}h^{-1}yr^{-1}$); K = the soil erodibility factor (in tonne (dimensionless).

The equation disclosed by Hurni[23], which is derived from spatial regression analysis [24] for Ethiopian environments, was used to calculate the Rainfall-Runoff Erosivity (R). It is based on data on mean annual rainfall that is currently available.

$$R = -8.12 + (0.562*P) (2)$$

where the Rainfall-Runoff (R) is The mean annual rainfall in millimetres is the erosivity factor, P. For 31 years, historical rainfall data were gathered for this investigation (1988–2019). Erodibility of soils is the scientific term for a soil's susceptibility to erosion. For a typical condition of bare soil that has recently been tilled up-and-down on a slope with no conservation practises and a slope of 5 to 22 metres, the soil erodibility factor (K) is the mean annual rainfall soil loss per unit of R [25]. The rate of soil loss per unit of R-factor on a unit plot is how Renard et al.[26] defined the K-factor. The range of K is 0 to 1, with 0 denoting soils with the least vulnerability to water erosion and 1 denoting soils with the greatest susceptibility [26, 27]. Regardless of the equivalent high content in the sand and clay fractions, soils typically become low erodible if the silt percentage is low. For each soil type, the ERFAC (Proposed Alternative Soil Erodibility Factor), a nonlinear regression equation, is used to calculate the K-factor for soil. Eq. 3 was designed for areas with a lack of data on organic matter.

$$\mathrm{ERFAC(K)} = \mathrm{a}\left(\frac{\%\mathrm{silt}}{\%\mathrm{sand} + \%\mathrm{clay}}\right)^{\mathrm{b}} (3)$$

Where, ERFAC: Proposed Alternative Soil Erodibility Factor, % silt = silt content of the soil, %clay = %clay content of the soil, % sand = % sand content of the soil, a = 0.32, and b = 0.27 a and b are factors obtained from regression coefficient.

The cover-management factor was generated from the Landsat 8 satellite image of January 2019 through the Normalized Difference Vegetation Index (NDVI). Since the C factor ranges from 0 (full cover) to 1 (bare land) and the NDVI values range from 1 (full cover) to 0 (bare land), the calculated NDVI values were inverted using (Eq. 4)[28].

$$C = exp[-\alpha.\frac{NDVI}{\beta - NDVI}](4)$$

Where: C is Cover management factor exp is exponent, NDVI is Normalized Difference Vegetation Index α, β: Parameters that determine the shape of the NDVI-C curve an α-value of 2 and a β-value of 1 seem to give reasonable results. The other factors calculated in our model approach were the topographic factor (LS) and anthropogenic soil erosion control practice factor (P). LS is the factor that expresses the effect of local topography on soil erosion rate, combining the effects of slope length (L) and slope steepness (S). Thus, LS is the predicted soil loss ratio per unit area from a field slope from a 22.1 m long, 9% (5.16°) slope under otherwise identical conditions[29]. L factor and S factor are usually considered together. Both GIS and remote sensing techniques were applied to access the LS factor in the RUSLE equation using the digital elevation model (DEM)[30]. The LS factor was calculated by multiplying L and S factors together (Moore and Burch, 1986) in a raster calculator in the ArcGIS platform with the help of the following equation:

$$\mathrm{LS} = \mathrm{POW}\left(\mathrm{FA}*\frac{\mathrm{CS}}{22.13}, 0.4\right)*\mathrm{Pow}\left(\sin\left(\mathrm{SD}*\frac{0.01745}{0.09}, 1.4\right)\right)*1.4(5)$$

LS = Slope Length and steepness factor, CS = Cell Size, Pow is Power, SD = is a slope in degree. The anthropogenic soil erosion control practice (P) factor is the most important parameter in the RUSLE method, and it is a dimensionless factor[31]. Defined the P factor as the ratio of soil loss in a particular support practice to the corresponding soil loss with up and downslope cultivation. P-value ranges from 0 to 1, where the value 0 indicates a good erosion-resistant facility made by man and the value 1 indicates an absence of an erosion-resistant facility. The P values were assigned by delineating the land into agricultural, forest, grass, and shrub and built-up land-use classes using Landsat 8 OLI satellite image classification.

The LULC map of the watershed was broadly categorized into agricultural and Non-agricultural Land uses, and a P value of 1 was assigned for Non-agricultural Land uses. As it was suggested by Wischmeir and Smith [32], Belayneh et al.[33] the agricultural land use was reclassified into 6 classes based on the slope (%) of the land, and the respective P-value for each class was assigned. Accordingly, the P-value of the agricultural lands with slope of 0–5% (0.11), 5–10% (0.12), 10–20% (0.14), 20–30% (0.19), 30–50% (0.25), 50–100%(0.33), 0-100%(1) was assigned. The classified agricultural land use map based on slope and Non-agricultural land use maps were overlaid after converting into vector format and assigning respective P-values. Finally, the overlaid map was converted into a raster format with a 30-m pixel size using its P-value to make it suitable for pixel-by-pixel overlay analysis to estimate soil erosion[33].

2.4 RUSLE model performance assessment and Validation of the result

The logarithmic form, and multiple linear regressions were applied to examine the relationships among all factors and the effects on the soil erosion rate. Thus, the multiple linear regressions equation (equations 6–8) (Pavisorn., et al.,2019).

$$\ln(A) = \ln(R \times K \times LS \times C \times P) \quad (6)$$

$$\ln(A) = \ln(R) + \ln(K) + \ln(LS) + \ln(C) + \ln(P) \quad (7)$$

$$\ln(A) = \beta 0 + \beta i(\ln R) + \beta j(\ln K) + \beta k(\ln LS) + \beta l(\ln C) + \beta h(\ln P) \quad (8)$$

Where ln(A) is the logarithm of soil erosion rate, ln(R, K, LS, C, and P) denotes the logarithmic value of the input factors in the RUSLE model, β0 is the intercept of soil erosion rate (constant term), and βi–h is the estimated regression coefficient of each explanatory variable. Different units of the input factors are reflected through the standard coefficient (β) in Eq. (15). The characteristics of multiple linear regression in logarithmic form can be explained as follows: if one of the factors in the RUSLE model increases by 1% in standard deviation, then βi–k percent of the standard deviation leads to an increased value of soil erosion rate (A).

The validity of the model outputs was checked based on empirical evidence from the RUSLE model and hydrological scientific model validation approach. In addition, a series of field observations were carried out to identify the most erosion-prone areas. In supporting these steps, the color printed model output for the soil erosion severity map was used in the field to check the level of soil erosion risk on the ground and compared the model result to the actuality of soil erosion features on the ground; the ground truth method which is a field verification of sampled locations from the produced soil loss map cross-checked with ground truth data showing the percentage of the checked points that matched the ground truth. The findings of the RUSLE model results were verified through the field observation, and deep erosion in zones of high to the extremely high-risk level of soil loss was confirmed. Field observation was supported by taking photographs and Google Earth images of different soil erosion features [34]. In addition, focus group discussions were used to compare and validate the soil erosion map result with what watershed communities perceived about each erosion factor and the resulting soil loss in the Midhagdu's watershed.

2.5 Identification of Soil Erosion Risk Area for Management Priority

Watershed management requires scientific knowledge of resource information, expected erosion maps, and priority class of raster-based grid cell level soil loss potential map and micro-watersheds for conservation planning[35]. Identifying soil erosion risk areas for management priority was accomplished in two approaches. The first approach was raster-based grid cell level soil loss potential map classification and prioritization, and the second was micro-watersheds level erosion risk area mapping and prioritization for management[36]. To identify soil erosion risk-prone area and management prioritization, the RUSLE model grid cell-based soil loss potential map of the Midhagdu watershed area was classified, and secondly, approaches of micro-watersheds erosion risk area mapping and prioritization for management was applied within Midhagdu's watershed.

In this procedure, the whole watershed was classified into 28 micro watersheds. The mean soil loss value of each micro watershed was estimated after extraction from the soil loss map of the entire watershed based on [36]. The mean annual soil loss of each micro watershed and their corresponding soil erosion risk level was registered in the vector map of each micro watershed. Each micro watershed's management priority level was assigned to its mean soil loss value and soil erosion risk levels[36]. Finally, soil erosion risk management options priority levels were obtained to support the spatial planning and implementation of soil erosion risk management options at micro watershed levels. The highest soil erosion risk management options priority rank was given for the area with the highest mean annual soil loss value and the highest soil erosion risk levels and vice versa[37].

3 Results And Discussion

3.1 Soil Erosion Factors and Thematic Map

3.1.1 Rainfall Erosivity (R) Factor

Between 1988–2019, the Midhagdu watershed experienced mean annual rainfall at six meteorological stations ranging from 87.87 to 92.37 mm yr-1. The Midhagdu watershed's estimated rainfall-runoff erosivity (R)factor ranged from 41.2649 MJ mm per year to 43.793 MJ mm per year and indicated that the distribution of precipitation and its corresponding rainfall-runoff erosivity was uneven in the study area (Figs. 1 and 2A).

3.1.2 Soil Erodibility (K) Factor

The results revealed that the study area's soil erodibility factor (K) ranges from 0.26 to 0.31 t ha^{-1} MJ^{-1} $mm^{-1}$with an annual average of 0.29 t ha^{-1} MJ^{-1} mm^{-1} (Fig. 2B). The minimum soil erodibility (0.26 t ha^{-1} MJ^{-1} mm^{-1}) factors imply less prone to soil erosion. On the other hand, the study area's maximum soil erodibility factor (0.31 t ha − 1 MJ − 1 mm − 1) showed that the watershed area is highly susceptible to erosion. The high K-factor value soil types are naturally more prone to soil erosion due to their physical structure, texture, permeability, and organic matter content. These results indicated that about 67.41% of the study area has a K-factor value of 0.31 and 0.30 for the soil types Eutric cambisols and Eutric fluvisols, respectively, which is considered high due to having low permeability, organic matter, and imperfect drainage. At the same time, K-factor values of 0.27 and 0.26 for Leptosols and Haplic xerosols, respectively, were considered lower susceptibility to soil erosion due to having acceptable soil permeability and moderately well drainage (Table 1).

Table 2
Soil type and soil texture percentage of the study area

No	soil type	Soil texture (%)			Km^2	Area Share (%)	Calculated
		Clay (%)	Silt (%)	Sand (%)			K-value (soil erodibility factor)
1	Leptosols	21	36	43	32.21	59	0.27
2	Eutric ambisols	24	46	30	14.06	26	0.31
3	Eutric Fluvisols	26	44	30	3.64	7	0.30
4	Haplic Xerosols	54	31	15	4.40	8	0.26

3.1.3 Topography (LS) Factor

The Midhagdu watershed's LS factor values, which ranged from 0 to 220.512, were dispersed after being derived from DEM data using GIS and remote sensing methods (Fig. 2C). Specifically in the first Order River, the low LS factor value is primarily found along the river valley. Mountainous places with ridgelines and steep terrain tend to have higher LS factor values.

3.1.4 Land Cover and Management (C) Factor

The estimated cover management factor produced results ranging from 0.21 to 0.87. (Fig. 2D). The study area's soil erosion will be reduced to 87 percent of what it would have been under continuous conditions to the highest cover management factor (0.87).

3.1.5 Anthropogenic soil erosion control practices (P) Factor

The conservation practise factor represents the relationship between soil erosion from land treated with a particular conservation strategy and its equivalent soil loss from upslope and downslope tillage[38]. The kind of conservation measure used can influence P-value. The land was divided into different land-use groups, including agricultural, forested, grassy, shrubby, and built-up areas, to get the P values. Moreover, using GIS software to overlay land use and slope maps, the farmland was classified into six slope classes. The P-value for this study therefore ranged from 0.11 to 1 (Fig. 2E). Minimum (0.11) P values indicate a moderated erosion-resistant facility made by a man. In contrast, the maximum (1) P-value indicated an absence of an erosion-resistant facility in the study area. The estimated conservation practice values range from 0.11 in cultivated land with a slope < 5–1% in other land use/covers except agricultural land uses.

3.2 Annual Soil Erosion Rate and Risk Analysis of Midhagdu Watershed

The mean annual soil loss of the Midhagdu watershed resulted in being 48.5 ton ha^{-1} $year^{-1}$ ranging from 0 to 1505.4 ton ha^{-1} $year^{-1}$ with a standard deviation of 78 ton ha^{-1} $year^{-1}$. The maximum soil loss was recorded only in a one-pixel area with a dimension of 30m*30m (0.09 ha). The total annual soil loss of the study area was 2,634,403 tons yr^{-1}. Spatial distribution of the study area map result was shown that a high soil loss value was recorded at the drainage lines of the watershed and the upper part of the watershed at steep slopes in all directions of the watershed (Figs. 3). This may be due to high land slopes, and cultivation land was the dominant land use type. The study area was categorized into five soil erosion classes at the Midhagdu watershed level (Table 3). The major portion of the watershed (44%) falls under low soil erosion risk levels (< 11 t ha^{-1} $year^{-1}$). The areas with low slopes showed a low risk of soil erosion, located mainly in the valley area of the *Midhagdu* watershed. Soil erosion risk levels of (8%) fall under moderate soil erosion risk levels (11–18 t ha^{-1} $year^{-1}$). The area characterized by high soil erosion risk levels (18–30 t ha^{-1} $year^{-1}$) covers (7%) of the total study area. Very high soil erosion risk levels (30–50 t ha^{-1} $year^{-1}$) cover (8%) of the total *Midhagdu* watershed area. Similarly, 32% of the *Midhagdu* watershed experienced extremely high soil erosion risk levels of (> 50 t ha^{-1} $year^{-1}$), observed along drainage lines and high slope parts of the watershed. The study area's cell-based model soil erosion output classification indicated that about 52.24% of the *Midhagdu* watershed area falls under low to moderate soil erosion risk levels. In the same way, approximately 47.77% of the study area falls under high to extremely high soil erosion risk levels.

The result of this study is in agreement with the findings of previous studies done in the highlands of the country and around the study area on erosion rate [33, 39, 40]. [41] also reported 47 t ha^{-1} $year^{-1}$ mean annual soil loss for soil estimation loss conducted in the case of the Koga watershed. Similarly, Gezaheny et al.[37] estimated the soil loss rate from 2000 to 2016 and reported a mean erosion rate of 51.04 t ha^{-1} $year^{-1}$ and 34.26 t ha^{-1} yr^{-1}, respectively, in the case of the Gobele watershed at East Hararghe Zone. Ajanaw *et al.*[36] also reported that 38.7 t ha^{-1} yr^{-1} mean annual soil loss for potential soil loss estimation and erosion-prone area prioritization in Chereti Watershed, northern Ethiopia. In addition, [9] noted that 93 t ha^{-1} $year^{-1}$ mean annual soil loss for the Chemoga watershed is almost double higher than the estimated result of this study. On the contrary, [42]) reported relatively lower soil loss results at 23.7 t ha^{-1} $year^{-1}$ for Geleda watershed and [43] 24.3 t ha^{-1} $year^{-1}$ for the Gelana sub-watershed. This could be attributed to the watershed's highland mountainous and steep slope conditions. Soil loss rate at the watershed level is determined by the interplay of physical, hydrological, and land management practices [44].

3.3 Consistency and Validation of the Model Estimate

3.3.1 Multiple linear regression analysis

To test the model performance and the effect of each soil erosion risk factor on soil erosion risk distribution in the *Midhagdu* watershed, each soil erosion factor thematic map and soil loss map were transformed into natural logarithms in the Arc GIS platform map algebra function-Raster calculator. The mean values of the natural logarithm of each soil erosion factor and soil loss values of 28 observation sites were extracted using Zonal statistics in Arc GIS. The natural logarithmic mean values of each soil erosion factor and the resultant mean annual soil loss of 28 micro watersheds (28 numbers of observations sites) within the *Midhagdu* watersheds were used for SPSS 16 version. The natural logarithmic(ln) RUSLE soil erosion risk influencing factors (independent variables) and the resultant soil loss (dependent variable) data transformation analysis results showed that the average annual estimated soil erosion rate (A) had a significant correlation, and there was no multi-collinearity with each input factor of soil erosion ($P < 0.05$, $VIF < 10$) and it indicated that the impact of each input factor of the soil erosion on the annual soil erosion rate was significant. The results presented in (Table) show that the estimated standardized coefficients, (β) values ranging from 0.079to 0.893for multiple linear regressions of the average annual estimated soil erosion rate (A) and each input factor of soil erosion at 28 micro watersheds within the Midhagdu watershed as follows:

$$\ln(A) = 0.079 * \ln(R) + 0.120 * \ln(K) + 0.893 * \ln(LS) + 0.199 * \ln(C) + .539 * \ln(P)$$

The β values indicated that the relative influential strength of each input factor on the annual soil erosion rate. The LS-factor had the strongest influence on soil erosion rate (β = 0.893) followed by the other factors, P (β = 0.539), C (β = 0.199), K (β = 0.120), and R (β = 0.079) respectively.

Table 3
Standardized coefficients (β) for RUSLE model-independent factors

Independent Factors	Standardized Coefficients Beta,β	Sig	Collinearity Statistics	
			Tolerance	VIF
InR	0.079	0.036*	0.918	1.089
InK	0.120	0.004**	0.826	1.210
InLS	0.893	0.000***	0.715	1.399
InC	0.199	0.000***	0.811	1.233
InP	0.539	0.000***	0.965	1.036
*Level of significance α 0.05 (95%)				

The model performance assessment revealed that the correlation between the observed value of performance (soil loss) and the optimal linear combination of the independent variables (rainfall Erosivity, soil erodibility, topographic, crop and cover management, anthropogenic soil erosion control) was 0.987as indicated by multiple R; and the R-Square value of 0.974and Adjusted-R square value of 0.969. Thus, it can be interpreted as 97.4% of the variation in performance (soil loss) can be explained by the independent variables.

Table 4
RUSLE Model performance assessment (Table 16).

Model Summary										
Model	R	R Square	Adjusted R Square	Std. An error in the Estimate	Change Statistics					Durbin-Watson
					R Square Change	F Change	df1	df2	Sig. F Change	
1	0.987[a]	0.974	0.969	0.1334	0.974	167.50	5	22	0.000	1.930
a. Predictors: (Constant), InP, InR, InC, InK, InLS										
b. Dependent Variable: InA										

3.3.2 The hydrological scientific model result validation approach

The hydrological scientific model validation method [45] was used to check the validity and consistency of the model estimation by comparing it with that of previously published results[33, 39, 46]. The result was compared against studies conducted in the Ethiopian Highland areas mainly with observed [47, 48] and estimated results [9, 39, 41, 46]. Some variations on previously reported results with this study estimates could be related to their respective site-specific variations in parameters.

3.3.3 Validation of RUSLE model results using ground truth erosion features

A color-printed soil erosion risk map was taken to the field to investigate the real-world phenomenon in the study site based on the graduated color assigned to the level of soil erosion risk area identified on the map. The validity of the soil erosion risk map was judged based on recorded erosion features at XY coordinates in the field and overlaid on top of the erosion risk map and calculated its accuracy [49, 50] by dividing the number of points laid on high, very high and extremely high regions of soil erosion map to the total points collected in the field and multiplied by hundred. Consequently, based on the generated map versus real-world phenomenon comparison for the model validation, 13 out of the 25 erosion sites fell within the extremely high-risk level of the RUSLE result, while 6 and 4of the erosion sites fell within the very high and high soil erosion risk areas respectively, out of 25 ground-truth erosion site 2 sites were fell in moderate erosion risk area in *Midhagdu* watershed soil map which makes the soil erosion prediction map 92 percent accurate with the real-world phenomenon.

3.3.4 Validation of RUSLE model result using Google earth

Google Earth has a Potential for quick, free, and accurate surveys that are particularly valuable to aid fieldwork. Fields at risk of erosion can be identified due to the inspection of Google Earth images of various dates[51]. And enough quality and accuracy in performing the erosion analysis due to detecting every contrasting detail in the terrain and comparing well with field mapped data can be achieved. Therefore, Google earth could identify where erosion had occurred. In this study, Google earth was used to locate erosion features in the study area where the RUSLE model located soil erosion has existed.

3.3.5 Validation of the RUSLE model using focus group discussion

As observed from the focus group discussion, all participants confirmed that soil erosion is a major problem in the *Midhagdu* watershed. According to the participants, the watershed is characterized by high topography, flooding and surface soil removal, high soil susceptibility to water erosion, deforestation, less land cover, and less human support for soil, water, and forest protection management. All these factors contribute to soil erosion in the watershed. The group suggested that all the elements of soil erosion should be managed to minimize the combined effect of the factors on soil erosion, which resulted in the very high rate of gully erosion, farmland bisected by huge soil erosion, shallow soils and rock outcrops, diminished soil moisture. Water resources decrease even in a swampy area, and the groundwater becomes lost quickly due to high ground and water erosion that creates low productivity and production from time to time in the *Midhagdu* watershed.

4 Conclusion

Soil erosion by water is among the most challenging and continuous environmental problems in the highlands of Ethiopia. In order to establish the distributions of soil erosion risk variables, calculate yearly soil erosion rates, and map out erosion hazards to prioritise management alternatives. The Midhagdu Watershed experienced issues with water and soil erosion. For many years, it has been challenging to quantify the quantity of soil erosion that causes land degradation at the watershed and micro watershed levels. Soil erosion models are useful to estimate soil loss and runoff rates at watershed and micro watersheds levels, plan land management strategies, provide relative soil loss indices, guide research, government policy, and systems on soil and water conservation practices.Estimating soil loss and identifying the critical areas for the intervention of best management options and techniques in the watershed is central to the success of soil and water conservation and management programs.

This study notably concluded that the use of Landsat 8 OLI and SRTM-DEM, besides the exploitation and extraction of World Climate and digital soil map databases, helped overcome the limited availability of complete and pertinent data relating to rainfall and soil respectively. The study identified the distributions of soil erosion risk factors in the *Midhagdu* watershed, estimated the soil erosion rate of the watershed, and prioritized soil erosion risk management options for soil conservation using soil loss risk levels in its 28 micro watersheds for effective soil and water conservation and watershed management planning using RUSLE model in combination with Geographic Information Systems and remote sensing techniques. It was learned that the RUSLE model, in combination with GIS and RS, was designed to develop the soil loss map and identify the areas of highest erosion risk and where conservation measures and soil erosion risk management options are demanded.

Different parts of the *Midhagdu* watershed reveal that the soil loss amount, soil erosion risk, and their extents varied. The grid cell-based model output indicated that mean annual soil losses of the *Midhagdu* watershed ranged from 0 in plain areas to 1504 t ha^{-1} $year^{-1}$ in the steep slope area of the *Midhagdu* watershed, with an average soil loss of 48.5 t ha^{-1} $year^{-1}$. The grid cell-based model output generated at the *Midhagdu* watershed level revealed that 52.24% (28.37 Km^2 out of 54.3 km^2) of the *Midhagdu* watershed falls in low to moderate soil erosion levels and 47.76% (25.94 km^2 out of 54.3 km^2) fall under extremely high soil erosion risk level at *Midhagdu* watershed level. The total annual soil loss from the entire watershed area of 54.3 km^2 was about 2,634,403 tons per year. Moreover, this portion of the watershed is dominated by inter-hill valleys where agriculture is practiced in the relatively sloppy areas that initiate soil loss. The combined effect of all the factors leads to a high rate of soil erosion. Consequently, large-scale expansion of agricultural land has been taking place over the last few decades through deforestation, leading to severe soil erosion.

RUSLE model performance evaluations using SPSS in 28 micro watersheds showed that the area's topography was a major threat that influenced soil and water erosions, followed by anthropogenic soil erosion control practices, crop and cover management practices, and soils erodibility factor and rainfall-runoff factor respectively. The soil erosion indicators' confirmation and validation of threats through the document review of previous studies, field observation, Google Earth inspections, and focus group discussions demonstrated that the soil erosion risk is real in the study area. Indeed, the erosion of the soil led to the soil and water washing away, groundwater depletion, shallow soils, soil moisture depletion including the dry-up of the swampy area, farmlands and riverbanks were turned into gullied lands with deforested, bare, mother-rocks exposed and reduced soil productivity and productions in the Midhagdu watershed.

References

1. J. Boardman, J. Poesen, and R. Evans, "Socio-economic factors in soil erosion and conservation," Environmental Science & Policy, vol. 6, pp. 1–6, 2003.
2. L. Montanarella, D. Pennock, N. McKenzie, M. Badraoui, V. Chude, I. Baptista, *et al.*, "World's soils are under threat," SOIL Discussions, vol. 2, pp. 1263–1272, 2015.
3. J. Poesen, "Soil erosion in the Anthropocene: Research needs," Earth Surface Processes and Landforms, vol. 43, pp. 64–84, 2018.
4. S. Rasool, S. Gaikwad, and P. Saptarshi, "Soil erosion assessment in Sallar Wullarhama watershed in the Lidder catchment of Jammu and Kashmir using, USLE, GIS and remote sensing," International Journal of Advanced Engineering Research and Studies, vol. 3, pp. 46–54, 2014.

5. D. Chalise, L. Kumar, and P. Kristiansen, "Land degradation by soil erosion in Nepal: A review," Soil Systems, vol. 3, p. 12, 2019.
6. D. Chalise, L. Kumar, V. Spalevic, and G. Skataric, "Estimation of sediment yield and maximum outflow using the IntErO model in the Sarada river basin of Nepal," *Water*, vol. 11, p. 952, 2019.
7. M. Wynants, C. Kelly, K. Mtei, L. Munishi, A. Patrick, A. Rabinovich, *et al.*, "Drivers of increased soil erosion in East Africa's agro-pastoral systems: changing interactions between the social, economic and natural domains," Regional Environmental Change, vol. 19, pp. 1909–1921, 2019.
8. T. Chen, R.-q. Niu, P.-x. Li, L.-p. Zhang, and B. Du, "Regional soil erosion risk mapping using RUSLE, GIS, and remote sensing: a case study in Miyun Watershed, North China," Environmental Earth Sciences, vol. 63, pp. 533–541, 2011.
9. W. Bewket and E. Teferi, "Assessment of soil erosion hazard and prioritization for treatment at the watershed level: a case study in the Chemoga watershed, Blue Nile basin, Ethiopia," Land degradation & development, vol. 20, pp. 609–622, 2009.
10. S. Jemai, A. Kallel, B. Agoubi, and H. Abida, "Soil erosion estimation in the arid area by USLE model applying GIS and RS: Case of Oued El Hamma catchment, south-eastern Tunisia," Journal of the Indian Society of Remote Sensing, vol. 49, pp. 1293–1305, 2021.
11. D. Pimentel and M. Burgess, "Soil erosion threatens food production," *Agriculture*, vol. 3, pp. 443–463, 2013.
12. G. Zeleke and H. Hurni, "Implications of land use and land cover dynamics for mountain resource degradation in the Northwestern Ethiopian highlands," Mountain research and development, vol. 21, pp. 184–191, 2001.
13. W. Bewket, "Land cover dynamics since the 1950s in Chemoga watershed, Blue Nile basin, Ethiopia," Mountain research and development, vol. 22, pp. 263–269, 2002.
14. X. Ma, Y. He, J. Xu, M. van Noordwijk, and X. Lu, "Spatial and temporal variation in rainfall erosivity in a Himalayan watershed," *Catena*, vol. 121, pp. 248–259, 2014.
15. G. Gebregziabher, D. A. Abera, G. Gebresamuel, M. Giordano, and S. Langan, *An assessment of integrated watershed management in Ethiopia* vol. 170: International Water Management Institute (IWMI). 2016.
16. Y. M. Tessema, J. Jasińska, L. T. Yadeta, M. Świtoniak, R. Puchałka, and E. G. Gebregeorgis, "Soil loss estimation for conservation planning in the welmel watershed of the Genale Dawa Basin, Ethiopia," *Agronomy*, vol. 10, p. 777, 2020.
17. A. Barakat, Z. Ouargaf, R. Khellouk, A. El Jazouli, and F. Touhami, "Land use/land cover change and environmental impact assessment in the béni-mellal district (morocco) using remote sensing and gis," Earth Systems and Environment, vol. 3, pp. 113–125, 2019.
18. A. Adediji, A. Tukur, and K. Adepoju, "Assessment of revised universal soil loss equation (RUSLE) in Katsina area, Katsina state of Nigeria using remote sensing (RS) and geographic information system (GIS)," Iranica Journal of Energy & Environment, vol. 1, pp. 255–264, 2010.
19. Y. Mukanov, Y. Chen, S. Baisholanov, A. C. Amanambu, G. Issanova, A. Abenova, *et al.*, "Estimation of annual average soil loss using the Revised Universal Soil Loss Equation (RUSLE) integrated with a Geographical Information System (GIS) of the Esil River basin (ERB), Kazakhstan," Acta Geophysica, vol. 67, pp. 921–938, 2019.
20. T. G. Feleke, P. D. Sharma, and D. T. Selfeko, "Assessing soil quality of Abargay Rangeland in Farta District, Amhara Regional State, Ethiopia," Journal of Soil Science and Environmental Management, vol. 10, pp. 46–57, 2019.

21. J. T. Abatzoglou, S. Z. Dobrowski, S. A. Parks, and K. C. Hegewisch, "TerraClimate, a high-resolution global dataset of monthly climate and climatic water balance from 1958–2015," *Scientific data*, vol. 5, pp. 1–12, 2018.
22. H. G. Abdo and R. M. Hassan, "Tartous, Syria," J Environ Geol Vol, vol. 2, 2018.
23. H. Hurni, "Erosion-productivity-conservation systems in Ethiopia," 1985.
24. G. J. Van Helden, P. S. Leeflang, and E. Sterken, "Estimation of the demand for electricity," Applied Economics, vol. 19, pp. 69–82, 1987.
25. R. Morgan, J. N. Quinton, and R. Rickson, "Modelling methodology for soil erosion assessment and soil conservation design: the EUROSEM approach," Outlook on Agriculture, vol. 23, pp. 5–9, 1994.
26. G. Foster, G. Weesies, K. Renard, D. Yoder, D. McCool, and J. Poster, "Support practice factor (P)," *Predicting soil erosion by water: A guide to conservation planning with the revised universal soil loss Equation (RUSLE)*, pp. 183–251, 1997.
27. Y. Farhan, D. Zregat, and I. Farhan, "Spatial estimation of soil erosion risk using RUSLE approach, RS, and GIS techniques: a case study of Kufranja watershed, Northern Jordan," Journal of Water Resource and Protection, vol. 5, p. 1247, 2013.
28. J. Van der Knijff, R. Jones, and L. Montanarella, *Soil erosion risk assessment in Italy*: Citeseer, 1999.
29. N. Kamuju, "Spatial identification and classification of soil erosion prone zones using remote sensing & GIS integrated 'RUSLE'model and 'SATEEC GIS system'," Int. J. Eng. Sci. Res. Technol, vol. 5, pp. 676–686, 2016.
30. G. Wang, H. Jiang, Z. Xu, L. Wang, and W. Yue, "Evaluating the effect of land-use changes on soil erosion and sediment yield using a grid-based distributed modeling approach," Hydrological Processes, vol. 26, pp. 3579–3592, 2012.
31. A. Pandey, V. Chowdary, and B. Mal, "Identification of critical erosion prone areas in the small agricultural watershed using USLE, GIS and remote sensing," Water resources management, vol. 21, pp. 729–746, 2007.
32. W. H. Wischmeier and D. D. Smith, *Predicting rainfall erosion losses: a guide to conservation planning*: Department of Agriculture, Science and Education Administration, 1978.
33. M. Belayneh, T. Yirgu, and D. Tsegaye, "Potential soil erosion estimation and area prioritization for better conservation planning in Gumara watershed using RUSLE and GIS techniques," Environmental Systems Research, vol. 8, pp. 1–17, 2019.
34. S. Ettazarini, M. El Jakani, and K. Najoui, "Assessment of soil loss risk using integrated remote sensing and geographic information system (GIS) techniques in the Argana Basin, Morocco," Am J Innovat Res Appl Sci, vol. 4, pp. 186–194, 2017.
35. G. Kiflu, "GIS-based conservation priority area identification in Mojo River watershed based on erosion risk," Mojo, Ethiopia, 2010.
36. A. Negese, E. Fekadu, and H. Getnet, "Potential soil loss estimation and erosion-prone area prioritization using RUSLE, GIS, and remote sensing in Chereti Watershed, Northeastern Ethiopia," Air, Soil and Water Research, vol. 14, p. 1178622120985814, 2021.
37. G. W. Woldemariam, A. D. Iguala, S. Tekalign, and R. U. Reddy, "Spatial modeling of soil erosion risk and its implication for conservation planning: the Gobele Watershed, East Hararghe Zone, Ethiopia," *land*, vol. 7, p. 25, 2018.
38. V. J. Markose and K. Jayappa, "Soil loss estimation and prioritization of sub-watersheds of Kali River basin, Karnataka, India, using RUSLE and GIS," Environmental monitoring and assessment, vol. 188, pp. 1–16, 2016.

39. M. Zerihun, M. S. Mohammedyasin, D. Sewnet, A. A. Adem, and M. Lakew, "Assessment of soil erosion using RUSLE, GIS and remote sensing in NW Ethiopia," Geoderma regional, vol. 12, pp. 83–90, 2018.
40. V. N. Balabathina, R. Raju, W. Mulualem, and G. Tadele, "Estimation of soil loss using remote sensing and GIS-based universal soil loss equation in the northern catchment of Lake Tana Sub-basin, Upper Blue Nile Basin, Northwest Ethiopia," Environmental Systems Research, vol. 9, pp. 1–32, 2020.
41. H. S. Gelagay and A. S. Minale, "Soil loss estimation using GIS and Remote sensing techniques: A case of Koga watershed, Northwestern Ethiopia," International Soil and Water Conservation Research, vol. 4, pp. 126–136, 2016.
42. T. Gashaw, T. Tulu, and M. Argaw, "Erosion risk assessment for prioritization of conservation measures in Geleda watershed, Blue Nile basin, Ethiopia," Environmental Systems Research, vol. 6, pp. 1–14, 2018.
43. B. A. Miheretu and A. A. Yimer, "Estimating soil loss for sustainable land management planning at the Gelana sub-watershed, northern highlands of Ethiopia," International Journal of River Basin Management, vol. 16, pp. 41–50, 2018.
44. T. Molla and B. Sisheber, "Estimating soil erosion risk and evaluating erosion control measures for soil conservation planning at Koga watershed in the highlands of Ethiopia," Solid Earth, vol. 8, pp. 13–25, 2017.
45. D. Biondi, G. Freni, V. Iacobellis, G. Mascaro, and A. Montanari, "Validation of hydrological models: Conceptual basis, methodological approaches and a proposal for a code of practice," *Physics and Chemistry of the Earth, Parts a/b/c*, vol. 42, pp. 70–76, 2012.
46. N. Haregeweyn, A. Tsunekawa, J. Poesen, M. Tsubo, D. T. Meshesha, A. A. Fenta, *et al.*, "Comprehensive assessment of soil erosion risk for better land use planning in river basins: A case study of the Upper Blue Nile River," Science of the Total Environment, vol. 574, pp. 95–108, 2017.
47. S. G. Setegn, B. Dargahi, R. Srinivasan, and A. M. Melesse, "Modeling of Sediment Yield From Anjeni-Gauged Watershed, Ethiopia Using SWAT Model 1," JAWRA Journal of the American Water Resources Association, vol. 46, pp. 514–526, 2010.
48. A. Subhatu, T. Lemann, K. Hurni, B. Portner, T. Kassawmar, G. Zeleke, *et al.*, "Deposition of eroded soil on terraced croplands in Minchet catchment, Ethiopian Highlands," International soil and water conservation research, vol. 5, pp. 212–220, 2017.
49. J. I. Amah, O. P. Aghamelu, O. V. Omonona, and I. M. Onwe, "A study of the dynamics of soil erosion using Rusle2 modeling and geospatial tool in Edda-Afikpo Mesas, South Eastern Nigeria," Pakistan Journal of Geology (PJG), vol. 4, 2020.
50. L. Bou-Imajjane and M. A. Belfoul, "Soil loss assessment in Western High Atlas of Morocco: Beni Mohand watershed study case," *Applied and Environmental Soil Science*, vol. 2020, 2020.
51. J. Boardman, "The value of Google Earth™ for erosion mapping," *Catena*, vol. 143, pp. 123–127, 2016.

Figures

Figure 1

Mean annual rainfall (mm/yr) for 31 years (1988-2019) of the study area

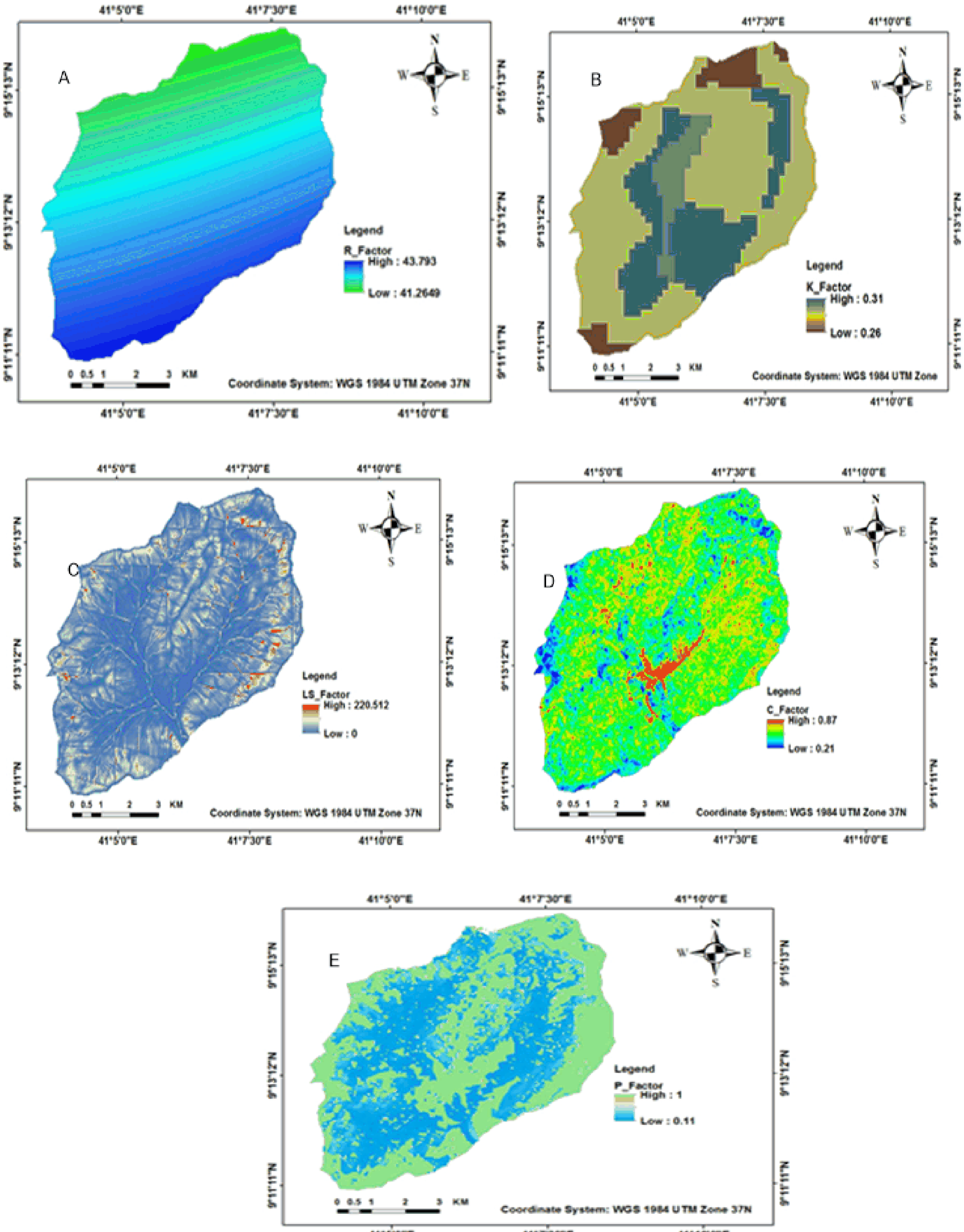

Figure 2

Spatial distribution of soil erosion risk influencing factors (A. Rainfall-runoff Erosivity (R), B. Soil erodibility (K), C. Slope Length-steepness (LS), D. Cover management (C), E. Anthropogenic soil erosion control practice (P)) of *Midhagdu* watershed.

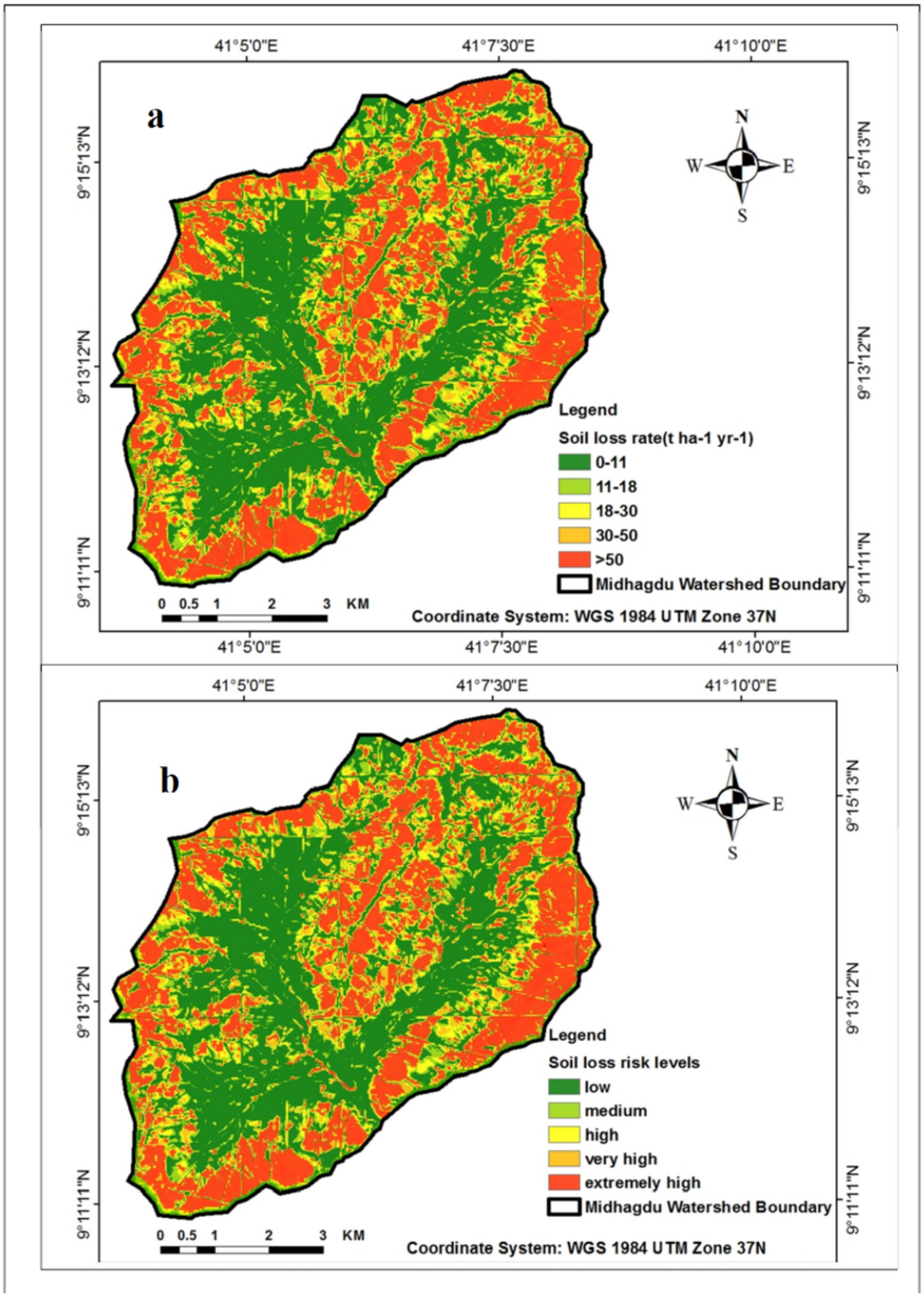

Figure 3

a. Spatial distribution of annual soil loss rate; b. soil erosion risk levels in the *Midhagdu* watershed